Zeolite Catalysis

How to cite:
International Edition: doi.org/10.1002/anie.202203859
German Edition: doi.org/10.1002/ange.202203859

Highly Selective Carbonylation of CH_3Cl to Acetic Acid Catalyzed by Pyridine-Treated MOR Zeolite

Xudong Fang, Fuli Wen, Xiangnong Ding, Hanbang Liu, Zhiyang Chen, Zhaopeng Liu, Hongchao Liu, Wenliang Zhu,* and Zhongmin Liu*

Abstract: The selective conversion of methane to high value-added chemicals under mild conditions is of great significance for the commercially viable and sustainable utilization of methane but remains a formidable challenge. Herein, we report a strategy for efficiently converting methane to acetic acid via CH_3Cl as an intermediate. Up to 99.3 % acetic acid and methyl acetate (AA + MA) selectivity was achieved over pyridine-pretreated MOR (MOR-8) under moderate conditions of 523 K and 2.0 MPa. Water, conventionally detrimental to carbonylation reaction over zeolite catalysts, was conducive to the production of AA in the current reaction system. In the 100 h continuous test with the MOR-8 catalyst, the average AA + MA selectivity remained over 98 %. AA was formed by carbonylation of methoxy groups within 8-membered rings of MOR followed by hydrolysis. This strategy provided an approach for highly efficient utilization of methane to oxygenates under mild reaction conditions.

Introduction

Methane, the main component of natural gas, shale gas and flammable ice, is not only a clean and inexpensive chemical feedstock with abundant reserves, but also an alternative energy vector to petroleum.[1] To date, methane has remained underutilized, with more than 90 % used as fuel for combustion in heating systems and only 5 % used for chemical synthesis.[2] Thus, the selective transformation of methane into high value-added chemicals, especially for oxygenates, is appealing and significant for sustainable chemistry and energy revolution. Currently, syngas-based route for methane conversion has been successfully commercialized.[2b] However, stringent reaction conditions and intricate operational processes are required, resulting in low energy efficiency and high costs in terms of capital and production.[3] The direct conversion of methane is considered to be potentially an environmentally friendly and economic route, and has been extensively studied for many years with great effort focusing on oxidative coupling of methane, partial oxidation of methane, co-activation of methane and carbon dioxide, and direct nonoxidative conversion of methane.[1b,4] Despite great progress in catalysts and reaction strategies for the direct conversion of methane, the low efficiency of methane utilization has remained unresolved due to the high C–H band energy (439.3 $kJ\,mol^{-1}$) and low polarizability of a methane molecule.[3,5] Currently methane derivatives, such as methyl halide,[6] are considered as significant intermediates for the utilization of methane, which has solved the difficult problem of methane activation. Therefore, it is essential to develop an efficient and ecofriendly route via methane derivatives to realize methane transformation into high value-added chemicals under mild conditions.

Acetic acid, one of the most important intermediates, has been widely used to produce vinyl acetate monomers, acetic anhydride, and acetic esters.[7] The selective conversion of methane to acetic acid has always attracted significant attention in practical production and academic research.[8] Recently, outstanding progress has been made in acetic acid production through direct methane oxidative carbonylation.[9] Specifically, Flytzani-Stephanopoulos et al. and Tao et al. reported that the Rh/ZSM-5 catalyst could efficiently transform methane to acetic acid with a production rate of acetic acid up to 31 $mol\,mol_{Rh}^{-1}\,h^{-1}$, which was higher than that any reported with metal-supported catalysts.[4b,8b,10] However, the selectivity to acetic acid remains low because acetic acid is more active than methane, resulting in the further conversion of acetic acid. Thus, it is significant to explore a new approach for transforming methane into acetic acid via methyl halides with higher efficiency and economics.

Methyl halide, a crucial intermediated chemical in the chemical industry, is produced readily from methane by halogenation or oxychlorination[6,11] and can be further converted to fuels and petrochemical commodities under moderate reaction conditions.[6,12] For example, up to 95 % olefin selectivity has been achieved catalyzed by SAPO-34 under reaction conditions of 723 K, 0.1 MPa in CH_3Br-to-olefins.[13] Recently, our team reported a novel route about aromatics production from the coupling of CH_3Cl and CO, obtaining up to 82.2 % aromatics selectivity and ca. 60 %

[*] X. Fang, Dr. F. Wen, X. Ding, H. Liu, Dr. Z. Chen, Z. Liu, Dr. H. Liu, Prof. W. Zhu, Prof. Z. Liu
National Engineering Research Center of Lower-Carbon Catalysis Technology, Dalian Institute of Chemical Physics, Chinese Academy of Sciences
Dalian 116023 (P. R. China)
E-mail: chliu@dicp.ac.cn
wlzhu@dicp.ac.cn
X. Fang, Dr. F. Wen, X. Ding, H. Liu, Dr. Z. Chen, Z. Liu, Prof. Z. Liu
University of Chinese Academy of Sciences
Beijing 100049 (China)

BTX (benzene, toluene, and xylene) selectivity.[14] Unfortunately, only a few investigations focusing on the conversion of methyl halide to oxygenates, especially for acetic acid, have been reported so far.[6] Thereinto, Zhou et al. and Bao et al. studied the carbonylation of methyl halide to acetic acid over $RhCl_3$-PPh_3-KI catalyst, achieving up to 99% acetic acid yield.[15] However, these studies focused on the multi-step method and noble metal homogeneous catalyst. To tackle this, a direct heterogeneous route for the transformation of methyl halide into acetic acid via CH_3Cl carbonylation was reported by Fujimoto, and approximately 94.6% selectivity of acetic acid and methyl acetate (AA + MA) was obtained over Rh/AC.[16] Nevertheless, this route still requires noble metal catalysts to obtain high selectivity of the target product.

Herein, we developed a new route for directly transforming CH_3Cl to acetic acid through a carbonylation reaction using acidic zeolites as the catalyst. Up to 99.3% (AA + MA) selectivity was achieved over pyridine-treated MOR (MOR-8) under reaction conditions of 523 K, 2.0 MPa, and 3000 mL g_{cat}^{-1} h^{-1}. During the 100 h continuous test, the MOR-8 catalysts exhibited excellent stability. Combined with multiple characterizations, 8-membered rings (8 MR) side pockets were shown to be the main active sites of acetic acid formation, while those in 12-membered rings (12 MR) promoted the formation of hydrocarbons. Moreover, the methoxy and acetyl groups were critical intermediate species in converting CH_3Cl. This work shed light on the tremendous potential of the halogen-mediated catalytic process for the conversion of methane to oxygenated compounds.

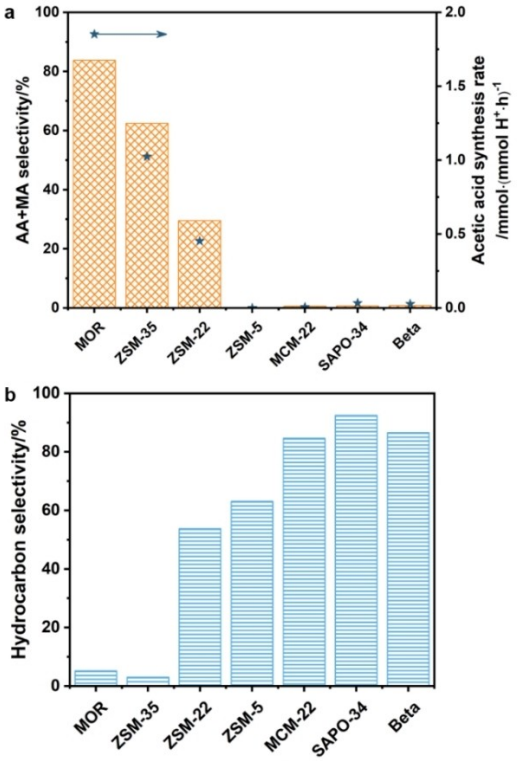

Figure 1. Catalytic performance over different zeolites. a) The selectivity to (AA + MA) and the acetic acid synthesis rate over zeolites with different topologies. b) The selectivity of hydrocarbons over zeolites with distinct topologies. Reaction conditions: 523 K, 2.0 MPa, P_{CO} = 500 kPa, P_{CH_3Cl} = 30 kPa, P_{H_2O} = 1.5 kPa, 2000 mL g_{cat}^{-1} h^{-1}, Ar as the balance gas. Note that the acetic acid synthesis rate is calculated based on the amount of acid. The data are obtained at the highest CH_3Cl conversion.

Results and Discussion

Acidic zeolites with different topologies, including MOR, FER, TON, MFI, MWW, CHA, and *BEA, are thoroughly selected for the chloromethane carbonylation reaction. The detailed structural properties and chemical information of acidic zeolites are exhibited in Figures S1–S3 and Tables S1, S2. Figure 1 illustrates how the product selectivity changes with different acidic zeolites under reaction conditions of 2.0 MPa, 523 K, and 2000 mL g_{cat}^{-1} h^{-1}. A significant difference in the selectivity to (AA + MA) and hydrocarbon can be observed ascribed to the different topologies of zeolites. As shown in Figure 1a, a higher acetic acid synthesis rate was obtained, catalyzed by the acidic zeolites with one-dimensional channels, such as MOR, ZSM-35, and ZSM-22, and the corresponding selectivities to (AA + MA) were 83.7%, 62.4% and 29.5%, respectively. The highest synthesis rate of acetic acid, as high as 1.85 mmol (mmol H^+ h)$^{-1}$, was achieved over HMOR. These results suggested that one-dimensional zeolites, especially MOR zeolites, were beneficial for forming acetic acid directly from CH_3Cl reacting with CO and H_2O. However, higher hydrocarbon selectivity was observed over the acidic zeolites with two- or three-dimensional structures, as shown in Figure 1b. Moreover, the selectivity to hydrocarbons over SAPO-34, MCM-22, Beta, and ZSM-5 are 92.5%, 84.7%, 86.6%, and 63.1%, respectively. Furthermore, the carbonaceous species extracted from the spent zeolites were analyzed by Gas Chromatography–Mass Spectrometry (GC-MS) following Guisnet's method.[17] As exhibited in Figure S4, typical coke species in carbonylation reaction, such as cyclopentenone, polymethyl benzaldehyde, and phenolic compounds, were observed on all zeolites, indirectly confirming that the carbonylation reaction occurred between CH_3Cl and CO over the acidic zeolites. Therefore, the difference in product distribution can be ascribed to a distinct confinement effect resulting from topology. Ulteriorly, acidic zeolites with a one-dimensional channel containing 8 MR or 10-membered rings (10 MR), were beneficial for the formation of acetic acid, whereas a complex channel structure favored the production of hydrocarbons. MOR zeolite was proven to be the most active catalyst among the acidic zeolites investigated for chloromethane conversion and used in subsequent investigations.

The variations in product distribution and the synthesis rates of acetic acid on HMOR at temperatures of 473 – 573 K and 2.0 MPa are depicted in Figure 2a. The selectivity to (AA + MA) increased achieving a maximum of 95.6% at 503 K, and then decreased with increasing reaction temperature. However, the formation rate of acetic acid gradually

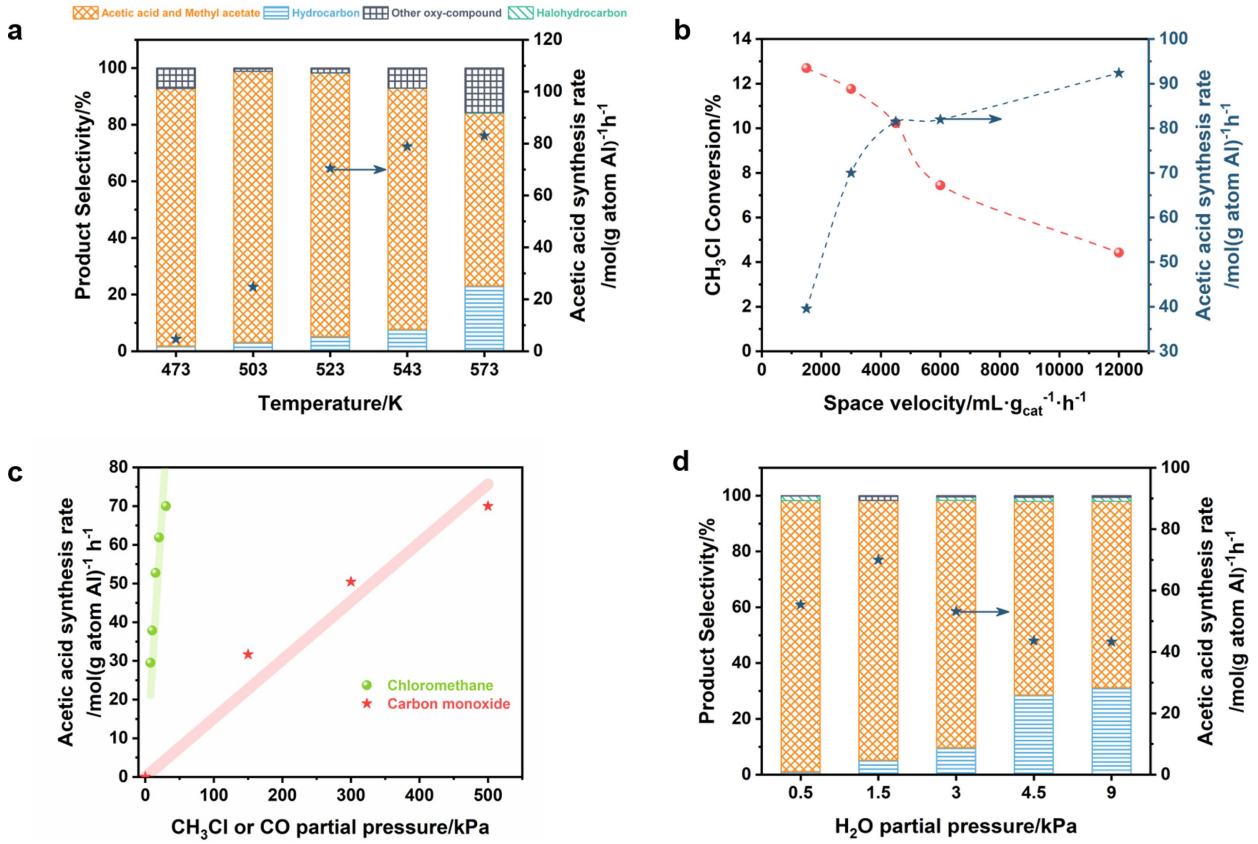

Figure 2. Catalytic performances in CH_3Cl carbonylation over mordenite. a) Acetic acid synthesis rate and product distribution at different reaction temperatures over HMOR. b) Acetic acid synthesis rate and CH_3Cl conversion over HMOR with different space velocity. c) Acetic acid synthesis rate over HMOR under different CH_3Cl or CO partial pressures. d) Acetic acid synthesis rate and product distribution over HMOR under different H_2O partial pressures. Reaction conditions: a) 2.0 MPa, $P_{CO}=500$ kPa, $P_{CH_3Cl}=30$ kPa, $P_{H_2O}=1.5$ kPa, 3000 mL g_{cat}^{-1} h^{-1}, Ar as balance gas; b) 523 K, 2.0 MPa, $P_{CO}=500$ kPa, $P_{CH_3Cl}=30$ kPa, $P_{H_2O}=1.5$ kPa, Ar as balance gas; c) 523 K, 2.0 MPa, ($P_{CH_3Cl}=7.5$–30 kPa, $P_{CO}=500$ kPa, $P_{H_2O}=1.5$ kPa) or ($P_{CH_3Cl}=30$ kPa, $P_{CO}=0$–500 kPa, $P_{H_2O}=1.5$ kPa), 3000 mL g_{cat}^{-1} h^{-1}, Ar as balance gas; d) 523 K, 2.0 MPa, $P_{CO}=500$ kPa, $P_{CH_3Cl}=30$ kPa, $P_{H_2O}=1.5$–9 kPa, 3000 mL g_{cat}^{-1} h^{-1}, Ar as balance gas. Note that the acetic acid synthesis rate is calculated based on the amount of Al atoms. The data are obtained in steady state.

increased from 4.7 to 70.4 mol (g atm Al)$^{-1}$ h^{-1}. This showed little change as the temperature increased further to 573 K. Meanwhile, the selectivity to hydrocarbons was also promoted at elevated temperatures, which was consistent with thermomechanical analysis (Figure S5). Thus, 523 K was selected as the optimal reaction temperature considering the selectivity to (AA + MA) and acetic acid synthesis rate. Note that the carbon and chlorine balances were 96.3 % and 93.8 %, respectively, obtained at 2.0 MPa, 523 K and 3000 mL g_{cat}^{-1} h^{-1} after 24 h. The effects of space velocity are illustrated in Figure 2b. An apparent increase in acetic acid synthesis rate was observed with increasing space velocity, reaching a maximum of 92.4 mol (g atom Al)$^{-1}$ h^{-1} at 12000 mL g_{cat}^{-1} h^{-1}. However, CH_3Cl conversion decreased from 12.7 % to 4.4 %. These results demonstrated that the high space velocity could inhibit the secondary reaction of acetic acid and methyl acetate.

The reactant partial pressure has an important influence on the conversion of CH_3Cl to acetic acid, as shown in Figure 2c. The synthesis rate of acetic acid almost increased linearly with increasing CH_3Cl pressure (7.5–30 KPa), exhibiting a positive correlation over the HMOR catalyst. In addition, according to the previous report, we speculated that the acetic acid synthesis rate showed little change under even higher CH_3Cl pressure due to the saturation of the surface methoxy groups.[18] Moreover, a decline in hydrocarbon selectivity (from 48.2 % to 8.5 %) was observed in Figure S6. These results suggested that a higher CH_3Cl pressure was beneficial for converting CH_3Cl to acetic acid and methyl acetate over HMOR. Furthermore, the formation of CH_3Cl-derived intermediate is considered as essential for CH_3Cl carbonylation. The influence of CO partial pressure on the formation of acetic acid was also examined, and the results are exhibited in Figure 2c. The synthesis rate of acetic acid monotonically increased with increasing CO pressure (0–500 kPa), revealing that the formation of acetic acid was closely related to CO pressure. Moreover, fewer hydrocarbons were produced at higher CO pressures (Figure S7). These results agreed with the findings from reactions between CO and small-molecule compounds.[14,19] Therefore, we deduced that the reaction of CO and CH_3Cl-

derived species might also be a significant step in forming acetic acid.

The effect of water content on the CH_3Cl carbonylation reaction is illustrated in Figure 2d. With increasing water partial pressure from 0.5 to 9 kPa, the selectivity of (AA + MA) decreased from 97.2 % to 66.8 %. The acetic acid synthesis rate increased first and then reached a maximum of 70.0 mol (g atom Al)$^{-1}$ h^{-1} at 1.5 kPa. Afterward, the acetic acid synthesis rate decreased with water partial pressure up to 9 kPa. Nevertheless, the hydrocarbon selectivity sharply increased from 5.2 % to 31.2 %. These results indicated that an appropriate amount of water favored the conversion of CH_3Cl and the formation of AA. Moreover, we speculated that the competitive occupation of active sites by excess water over HMOR zeolite inhibited the carbonylation of CH_3Cl and the dimerization and cyclization of hydrocarbons, leading to the increase of hydrocarbon selectivity based on our results and the previous reports.[20] However, more detailed studies are needed to certify the hypothesis in subsequent work.

The silicon to aluminum ratio (SAR) of zeolites has played an essential role in determining the catalytic performance in acidic catalytic reactions.[21] Therefore, a series of MOR zeolites with different SARs were employed in the chloromethane carbonylation reaction at 523 K, 2.0 MPa, and 3000 mL g_{cat}^{-1} h^{-1}. Figure 3a shows that the selectivity of (AA + MA) increased gradually (83.6 % to 93.0 %) with increasing SAR from 6.3 to 14.7, while the hydrocarbon selectivity significantly decreased from 14.2 % to 5.2 %. Concurrently, the synthesis rate of acetic acid monotonically increased, and up to 70.0 mol (g atm Al)$^{-1}$ h^{-1} was achieved over MOR-14.7. Thus, we concluded that a higher SAR was beneficial to the directional conversion of CH_3Cl to acetic acid. The XRD patterns, surface topography, and textural properties are displayed in Figures S8, S9 and Tables S2, which suggested that the samples with different SARs had similar physical properties. Proverbially, the SAR of zeolites can directly affect acidic properties. Although the acid content of the samples declined with increasing SAR, as shown in Figure S10, the ratio of Brønsted acid sites (BAS) in 8 MR to those in 12 MR increased from 0.3 to 2.0 (Figure S11 and Table S3). These results were in agreement with the results that MOR with higher SAR possessed much more BAS in 8 MR.[22] Interest-

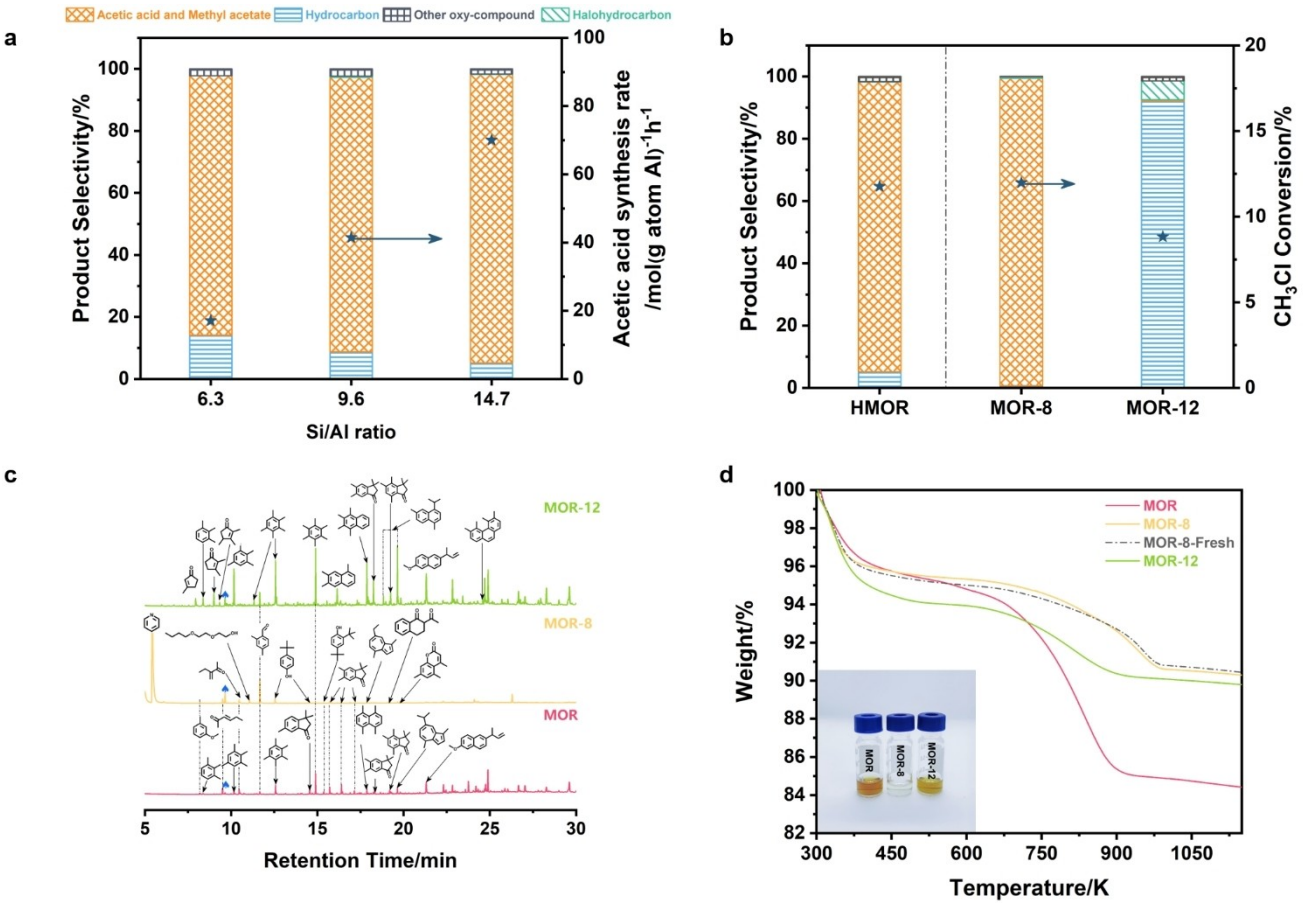

Figure 3. Effects of acidic properties on the chloromethane carbonylation reaction. a) Acetic acid synthesis rate and product distribution catalyzed by HMOR with different SARs. b) Acetic acid synthesis rate and product distribution catalyzed by HMOR with different acid distributions. c) GC-MS total ion chromatograms of the organic species extracted from spent catalysts with different acidic locations. d) Thermal analysis of spent catalysts with different acidic locations. Reaction conditions (a, b): 523 K, 2.0 MPa, P_{CO} = 500 kPa, P_{CH_3Cl} = 30 kPa, P_{H_2O} = 1.5 kPa, 3000 mL g_{cat}^{-1} h^{-1}. Note that the acetic acid synthesis rate is calculated based on the amount of Al atoms. The data are obtained in steady state.

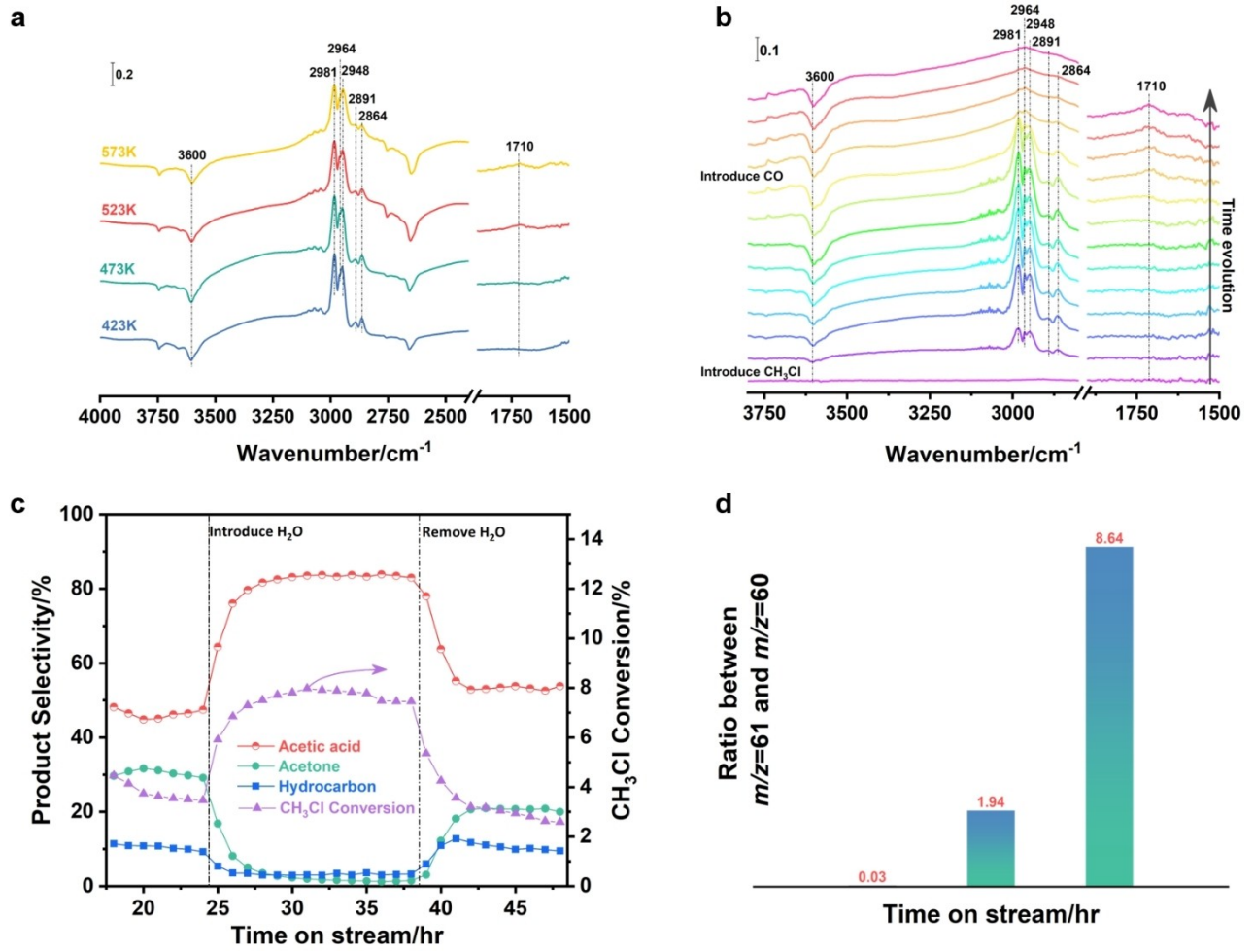

Figure 4. Catalytic performances in CH_3Cl carbonylation and in situ DRIFTs. a) In situ DRIFTs from CH_3Cl carbonylation over HMOR at different reaction temperatures. b) In situ DRIFTs from CH_3Cl carbonylation over HMOR with increasing time. c) The influence of water on catalytic performance over MOR. d) The ratio between $m/z=61$ and $m/z=60$ in acetic acid with D_2O co-feeding over MOR-8. Reaction conditions: a) 0.5 MPa, CO:CH_3Cl = 17:1 (molar ratio), 0.14 $g_{CH_3Cl}\,g_{cat}^{-1}\,h^{-1}$; b) 523 K, 0.5 MPa, CO:$CH_3Cl$ = 30:1 (molar ratio); c) 523 K, 2.0 MPa, P_{CO} = 500 kPa, P_{CH_3Cl} = 30 kPa, P_{H_2O} = 1.5 kPa or 0 kPa, 3000 mL $g_{cat}^{-1}\,h^{-1}$; d) 523 K, 2.0 MPa, P_{CO} = 500 kPa, P_{CH_3Cl} = 30 kPa, P_{H_2O} = 5.2 kPa, 3000 mL $g_{cat}^{-1}\,h^{-1}$.

ingly, the acetic acid synthesis rate was positively correlated with the proportion of BAS in 8 MR. Therefore, we preliminarily deduced that the acid sites in 8 MR might be the active centers of the CH_3Cl carbonylation reaction to acetic acid.

To understand the effect of acidic sites within the different channels of MOR zeolite on CH_3Cl carbonylation in-depth, the samples containing BAS solely in the 12 MR channel or 8 MR side pockets were prepared by ion-exchange or pyridine pre-adsorption (Supporting Information and Figure S12) and correspondingly denoted as MOR-12 and MOR-8, respectively. The textural and chemical properties of the samples are shown in Figures S13–S15. As shown in Figure 3b, (AA + MA) selectivity reaching 99.3 % was achieved over the MOR-8 catalyst. Nevertheless, up to 92.1 % selectivity of hydrocarbons was obtained catalyzed by MOR-12. These results demonstrated that the location of BAS played a decisive role in the formation of target products. Furthermore, the coke species trapped in MOR, MOR-8, and MOR-12 were analyzed via GC-MS. As seen in Figure 3c, the carbonaceous species in MOR-8 and MOR were the same containing methyl-substituted indanones, methyl-substituted benzaldehyde, and alkylphenol. However, the main carbonaceous species in MOR-12 were methyl cyclopentenone and polyaromatics. These results implied that the carbonylation of CH_3Cl mainly occurred on BAS in 8 MR side pockets. In contrast, BAS at 12 MR channels was responsible for forming of hydrocarbons from CH_3Cl or coupling CH_3Cl with CO.[6,23] Notably, methyl cyclopentenone is observed over MOR-12, which revealed BAS in the 12 MR channel also possessed the ability of coupling CH_3Cl with CO according to the previous literature.[14,19a,d] As shown in Figure 3d and Table S4, the amount of coke over MOR-12 (3.92 wt %) is higher than that over MOR-8 (0.46 wt %). Nevertheless, the MOR had the largest amount of coke (10.00 wt %). The difference in the amount of coke was possibly caused by the easy conversion of acetic acid or methyl acetate to coke during

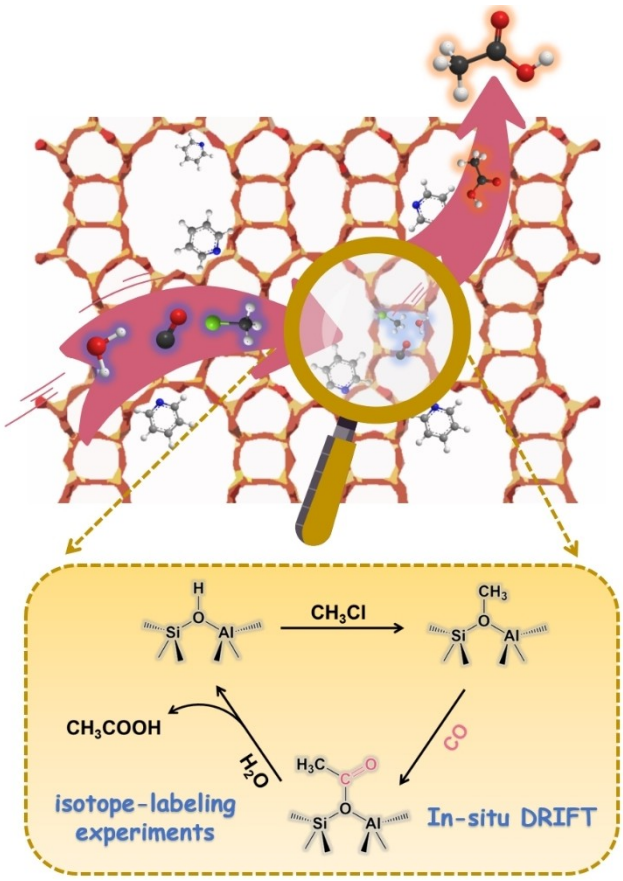

Figure 5. The proposed mechanism of CH_3Cl carbonylation over MOR-8.

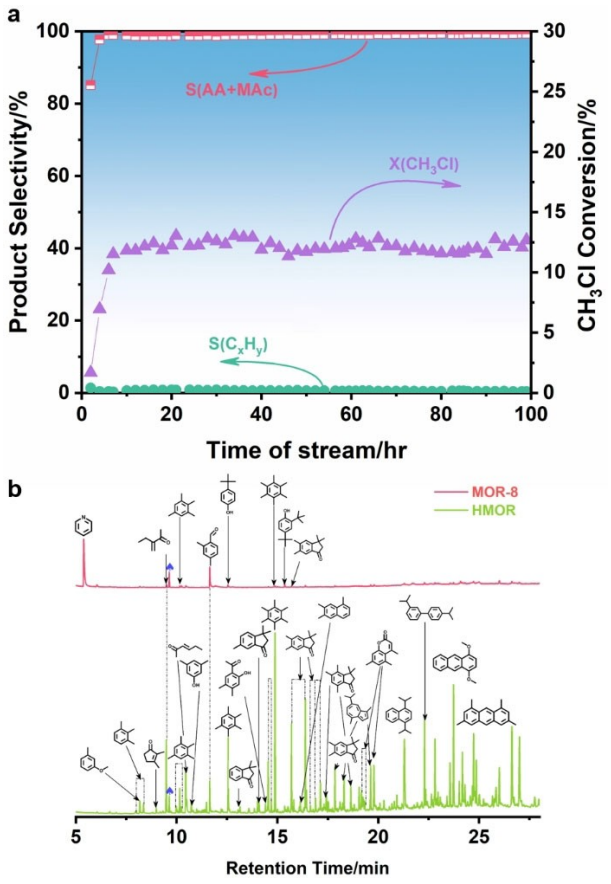

Figure 6. Stability of pyridine pre-adsorption mordenite on CH_3Cl carbonylation to acetic acid. a) Stability test for MOR-8. b) GC-MS chromatograms of organic materials retained over HMOR and MOR-8 after 100 h. Reaction condition: 523 K, 2.0 MPa, (HMOR) $P_{CO}=500$ kPa, $P_{CH_3Cl}=30$ kPa, $P_{H_2O}=1.6$ kPa; (MOR-8) $P_{CO}=500$ kPa, $P_{CH_3Cl}=30$ kPa, $P_{H_2O}=5.2$ kPa, 3000 mL g_{cat}^{-1} h^{-1}; the catalysts were collected at 100 h in chloromethane carbonylation.

the diffusion from 8 MR to 12 MR. Thus, it can be concluded that the CH_3Cl carbonylation reaction occurred mainly in 8 MR channels, while the coke species were produced in 12 MR channels.

To clarify the reaction mechanism of chloromethane carbonylation, the surface species that formed on HMOR were detected under different reaction temperatures at 1.0 MPa by in situ DRIFTs, as shown in Figure 4a. A negative peak at 3600 cm^{-1} is observed at 423 K due to the interactions of CH_3Cl and BAS. Simultaneously, bands appeared at 2981, 2964, 2948, 2891, and 2864 cm^{-1}. These observations agreed with the results obtained under different CH_3Cl pressures, as shown in Figure S16. Combined with our results and previous reports,[12] these peaks at 2800–3000 cm^{-1} were assigned to the methoxy groups resulting from the dissociation of CH_3Cl. Moreover, the intensity of the five peaks decreased gradually with increasing reaction temperature (423 to 573 K). Additionally, the peak at $\approx$1710 cm^{-1}, ascribed to the acetyl group ($-COCH_3$), was observed above 523 K and gradually increased with increasing temperature. These results indicated that the reaction included the formation and conversion of methoxy groups. Subsequently, the reaction process via different feeding methods was conducted, as illustrated in Figure 4b. After introducing CH_3Cl at 523 K and 0.5 MPa, the adsorption of CH_3Cl induced negative peaks at 3601 cm^{-1}, signifying that CH_3Cl interacted with BAS in HMOR. With time, the peaks of methoxy groups at 2989, 2981, 2964, 2948, 2891, and 2864 cm^{-1} appeared and were gradually enhanced. Moreover, the silver nitrate solution became turbid after passing into the tail gas (Figure S17). These results demonstrated that CH_3Cl initially adsorbed on BAS, forming methoxy groups and HCl. When the feed gas was changed to CO, the methoxy group peaks decreased until they disappeared. Simultaneously, the peak of acetyl groups at $\approx$1710 cm^{-1} was enhanced with reaction time. These observations revealed that the acetyl group is formed via the reaction CO and methoxy group. Therefore, the carbonylation reaction mechanism involved two key steps: the formation of methoxy groups by the dissociation of CH_3Cl, and then the formation of acetyl groups.

Based on the above results, the role of H_2O in the carbonylation of CH_3Cl was further studied, as shown in Figure 4c. Acetic acid and acetone were observed as the main products without water, implying that carbonylation

reactions of CH_3Cl with CO were successfully processed. Moreover, methanol was hardly observed, ruling out the possibility of methanol carbonylation to acetic acid. Afterward, acetone disappeared entirely with increasing CH_3Cl conversion and acetic acid selectivity once the appropriate amount of H_2O was introduced. These findings confirmed that H_2O could rapidly remove the acetyl groups to form acetic acid. As expected, upon cutting off H_2O again, acetone appeared immediately and increased gradually, accompanied by a decrease in CH_3Cl conversion and acetic acid selectivity. Therefore, it could be concluded that methanol was not the intermediate in CH_3Cl carbonylation, and the presence of water helped to complete the catalytic recycling, thereby accelerating the formation of acetic acid. Furthermore, D_2O was employed in chloromethane carbonylation to understand the formation of acetic acid. As shown in Figure 4d, acetic acid in the product collected at different times was analyzed by GC-MS. The signal intensity ratio between 61 and 60 gradually increased with prolonged time, which indicated that the acetyl groups reacted with D_2O to form acetic acid. Thus, it can be concluded that acetic acid can be formed via the hydrolysis of acetyl groups. Overall, the reaction mechanism is proposed, as shown in Figure 5, includes three steps: 1) CH_3Cl was adsorbed on BAS in MOR to form methoxy groups and HCl; 2) the methoxy groups reacted with CO to generate acetyl groups; 3) the acetyl groups were hydrolyzed by H_2O to form acetic acid.

MOR-8 was employed under the optimized conditions, as shown in Figure 6a. Unexpectedly, the average selectivity to (AA + MA) was over 98 % with approximately 12 % CH_3Cl conversion at 2.0 MPa and 523 K during 100 h, which was higher than that over the Rh/Ac (94.6 %), as reported by Fujimoto.[16] Moreover, the stability of MOR-8 was perfect, and higher than that of MOR during the 100 h, as illustrated in Figures 6a and S18. As expected, the color of spent MOR-8 was lighter than that of MOR (Figure S19). In addition, the carbonaceous species trapped over MOR-8 were 2,4-dimethyl benzaldehyde, 2,4-diisopropyl phenol, and 3,3,5,6-tetramethyl-1-indanone, and their amounts were much lower than those over HMOR as shown in Figures 6b and S20. Thus, selective poisoning of BAS in 12 MR channels, terminating the further transformation of acetyl groups generated on BAS of 8 MR side pockets into cokes, was an effective method for enhancing activity and lifetime.

Conclusion

In summary, a novel strategy capable of producing acetic acid via the carbonylation of CH_3Cl using acidic zeolites was proposed for the comprehensive utilization of methane. We first demonstrated that the coupling of CH_3Cl with CO and H_2O occurred over acidic zeolites especially one-dimensional with 8 MR or 10 MR. In particular, the high selectivity of (AA + MA) reaching 99.3 % could be obtained over MOR-8 under the optimized conditions, which was superior to that of Rh/AC under CH_3I-free conditions. The BAS in 8-MR has been proven to be the main active site for chloromethane carbonylation. Moreover, the reaction mechanism was proposed, including the chemical adsorption of CH_3Cl, the formation of acetyl groups, and the hydrolysis of acetyl groups. These findings would present enormous potential and advantages in the efficient and practical transformation of methane into oxygenates in the future.

Acknowledgements

We sincerely acknowledge the financial support from the National Natural Science Foundation of China (Grant Nos. 21972141, 21991094 and 21991090), the "Transformational Technologies for Clean Energy and Demonstration", Strategic Priority Research Program of the Chinese Academy of Sciences (Grant No. XDA21030100), the Dalian High Level Talent Innovation Support Program (2017RD07), and the National Special Support Program for High Level Talents (SQ2019RA2TST0016).

Conflict of Interest

The authors declare no conflict of interest.

Data Availability Statement

The data that support the findings of this study are available from the corresponding author upon reasonable request.

Keywords: Carbon Monoxide · Carbonylation · Chloromethane · Methane Conversion · Mordenite

[1] a) K. Huang, J. B. Miller, G. W. Huber, J. A. Dumesic, C. T. Maravelias, *Joule* **2018**, *2*, 349–365; b) X. Meng, X. Cui, N. P. Rajan, L. Yu, D. Deng, X. Bao, *Chem* **2019**, *5*, 2296–2325.

[2] a) X. Yu, V. L. Zholobenko, S. Moldovan, D. Hu, D. Wu, V. V. Ordomsky, A. Y. Khodakov, *Nat. Energy* **2020**, *5*, 511–519; b) A. I. Olivos-Suarez, A. Szecsenyi, E. J. M. Hensen, J. Ruiz-Martinez, E. A. Pidko, J. Gascon, *ACS Catal.* **2016**, *6*, 2965–2981.

[3] a) Y. Wang, *Joule* **2018**, *2*, 1399–1401; b) P. Schwach, X. Pan, X. Bao, *Chem. Rev.* **2017**, *117*, 8497–8520.

[4] a) Z. Jin, L. Wang, E. Zuidema, K. Mondal, M. Zhang, J. Zhang, C. T. Wang, X. J. Meng, H. Q. Yang, C. Mesters, F. S. Xiao, *Science* **2020**, *367*, 193–197; b) J. F. Wu, S. M. Yu, W. D. Wang, Y. X. Fan, S. Bai, C. W. Zhang, Q. Gao, J. Huang, W. Wang, *J. Am. Chem. Soc.* **2013**, *135*, 13567–13573; c) W. Huang, K. C. Xie, J. P. Wang, Z. H. Gao, L. H. Yin, Q. M. Zhu, *J. Catal.* **2001**, *201*, 100–104.

[5] a) P. Tang, Q. Zhu, Z. Wu, D. Ma, *Energy Environ. Sci.* **2014**, *7*, 2580–2591; b) Y. Liu, D. Deng, X. Bao, *Chem* **2020**, *6*, 2497–2514.

[6] R. Lin, A. P. Amrute, J. Perez-Ramirez, *Chem. Rev.* **2017**, *117*, 4182–4247.

[7] C. Tu, X. Nie, J. G. Chen, *ACS Catal.* **2021**, *11*, 3384–3401.

[8] a) R. A. Periana, O. Mironov, D. Taube, G. Bhalla, C. J. Jones, *Science* **2003**, *301*, 814–818; b) J. Shan, M. Li, L. F. Allard, S. Lee, M. Flytzani-Stephanopoulos, *Nature* **2017**, *551*, 605–608.

[9] K. Narsimhan, V. K. Michaelis, G. Mathies, W. R. Gunther, R. G. Griffin, Y. Roman-Leshkov, *J. Am. Chem. Soc.* **2015**, *137*, 1825–1832.
[10] Y. Tang, Y. Li, V. Fung, D. E. Jiang, W. Huang, S. Zhang, Y. Iwasawa, T. Sakata, L. Nguyen, X. Zhang, A. I. Frenkel, F. F. Tao, *Nat. Commun.* **2018**, *9*, 1231.
[11] a) G. Zichittella, V. Paunović, A. P. Amrute, J. Pérez-Ramírez, *ACS Catal.* **2017**, *7*, 1805–1817; b) M. Bilke, P. Losch, O. Vozniuk, A. Bodach, F. Schuth, *J. Am. Chem. Soc.* **2019**, *141*, 11212–11218.
[12] Y. X. Wei, D. Z. Zhang, Z. M. Liu, B. L. Su, *J. Catal.* **2006**, *238*, 46–57.
[13] P. Wang, L. Chen, J.-K. Guo, S. Shen, C.-T. Au, S.-F. Yin, *Ind. Eng. Chem. Res.* **2019**, *58*, 18582–18589.
[14] X. Fang, H. Liu, Z. Chen, Z. Liu, X. Ding, Y. Ni, W. Zhu, Z. Liu, *Angew. Chem. Int. Ed.* **2022**, *61*, e202114953; *Angew. Chem.* **2022**, *134*, e202114953.
[15] a) K. X. Wang, H. F. Xu, W. S. Li, C. T. Au, X. P. Zhou, *Appl. Catal. A* **2006**, *304*, 168–177; b) Y. F. Fan, D. Ma, X. H. Bao, *Catal. Lett.* **2009**, *130*, 286–290.
[16] T. Shikada, H. Yagita, K. Fujimoto, H. Tominaga, *Appl. Catal.* **1986**, *22*, 379–384.
[17] M. Guisnet, P. Magnoux, *Appl. Catal.* **1989**, *54*, 1–27.
[18] J. Qi, J. Finzel, H. Robatjazi, M. Xu, A. S. Hoffman, S. R. Bare, X. Pan, P. Christopher, *J. Am. Chem. Soc.* **2020**, *142*, 14178–14189.
[19] a) Z. Chen, Y. Ni, Y. Zhi, F. Wen, Z. Zhou, Y. Wei, W. Zhu, Z. Liu, *Angew. Chem. Int. Ed.* **2018**, *57*, 12549–12553; *Angew. Chem.* **2018**, *130*, 12729–12733; b) F. Wen, J. Zhang, Z. Chen, Z. Zhou, H. Liu, W. Zhu, Z. Liu, *Catal. Sci. Technol.* **2021**, *11*, 1358–1364; c) C. Wei, Q. Yu, J. Li, Z. Liu, *ACS Catal.* **2020**, *10*, 4171–4180; d) C. Wei, J. Li, K. Yang, Q. Yu, S. Zeng, Z. Liu, *Chem Catal.* **2021**, *1*, 1273–1290.
[20] a) P. Cheung, A. Bhan, G. J. Sunley, E. Iglesia, *Angew. Chem. Int. Ed.* **2006**, *45*, 1617–1620; *Angew. Chem.* **2006**, *118*, 1647–1650; b) K. De Wispelaere, C. S. Wondergem, B. Ensing, K. Hemelsoet, E. J. Meijer, B. M. Weckhuysen, V. Van Speybroeck, J. Ruiz-Martínez, *ACS Catal.* **2016**, *6*, 1991–2002.
[21] Q. Zhang, J. Yu, A. Corma, *Adv. Mater.* **2020**, *32*, 2002927.
[22] B. Lu, T. Kanai, Y. Oumi, T. Sano, *J. Porous Mater.* **2007**, *14*, 89–96.
[23] D. K. Murray, T. Howard, P. W. Goguen, T. R. Krawietz, J. F. Haw, *J. Am. Chem. Soc.* **1994**, *116*, 6354–6360.

Manuscript received: March 17, 2022
Accepted manuscript online: May 30, 2022
Version of record online: ■■, ■■

Research Articles

Zeolite Catalysis

X. Fang, F. Wen, X. Ding, H. Liu, Z. Chen, Z. Liu, H. Liu,* W. Zhu,* Z. Liu e202203859

Highly Selective Carbonylation of CH_3Cl to Acetic Acid Catalyzed by Pyridine-Treated MOR Zeolite

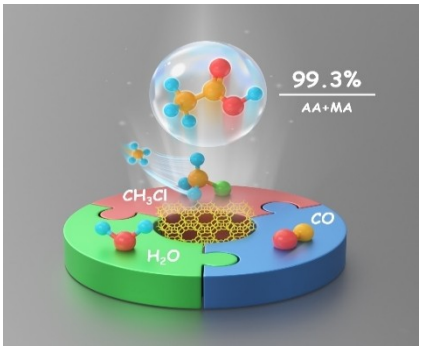

An innovative reaction strategy for the transformation of methane into acetic acid via CH_3Cl carbonylation over H-zeolites is reported. A 99.3% acetic acid (AA) and methyl acetate (MA) selectivity was obtained over pyridine-pretreated MOR at 523 K and 2.0 MPa. This strategy enables efficient conversion of methane into oxygenates under mild conditions.